

## NUMERICAL SIMULATION OF A MACRO-QUANTUM EXPERIMENT: OSCILLATING WAVE PACKET

LAURENT NOTTALE\* and THIERRY LEHNER†

*LUTH, CNRS, Observatoire de Paris-Meudon  
5 Place Janssen, F-92195 Meudon Cedex, France*

*\*laurent.nottale@obspm.fr*

*†thierry.lehner@obspm.fr*

Received 11 October 2011

Accepted 23 March 2012

Published 3 May 2012

We perform numerical simulations of a new proposal of laboratory experiment that would allow the transformation of a classical fluid into a quantum-type (super)fluid through the application of a generalized quantum potential. This quantum potential is simulated by using a real time retroactive loop involving a measurement of density, a calculation of the potential in function of the measured density, then an application of the calculated potential through a classical force. This general experimental concept is exemplified here by the case of a nonspreading oscillating wave packet in a harmonic oscillator potential. We find signatures of a quantum-like behavior which are stable against various perturbations. Finally, the feasibility of a realization of this concept in an actual plasma experiment is analyzed.

*Keywords:* Fluid dynamics; quantum fluid; quantum potential; numerical simulations.

PACS Nos.: 47.11.+j, 67.90.+x, 02.60.Cb, 02.70.Bf.

### 1. Introduction

One of us has recently proposed a new general concept of macroscopic quantum-type laboratory experiments.<sup>1-3</sup> It consists of applying, through a real time retroactive loop, a generalized quantum potential on a classical system. Indeed, one can show that the system of equations (Euler equation and continuity equation) that describes a fluid in irrotational motion subjected to such a generalized quantum potential, that reads  $Q = -2\mathcal{D}^2\Delta\sqrt{\rho}/\sqrt{\rho}$  in terms of the density  $\rho$ , is equivalent to a generalized Schrödinger equation. In this derivation, the quantum potential is no longer founded on the quantum Planck's constant  $\hbar$ , but on a new constant  $\mathcal{D}$  which can take any macroscopic value. While it would be impossible with present days technology to simulate standard quantum effects by this method because of the smallness of  $\mathcal{D}$ , which is given by  $\mathcal{D} = \hbar/2m$  in standard quantum mechanics, the use of a macroscopic value for this constant nevertheless preserves some of the properties of a

quantum-like system. Namely, its density distribution is given by the square of the modulus of a complex function which is solution of a Schrödinger equation. Therefore such a system is expected to exhibit some quantum-type, superfluid-like macroscopic properties (though certainly not every aspects of a genuine quantum system).

In the present paper we validate this concept by numerical simulations of a fluid subjected to such a generalized quantum force, as an anticipation of a future real laboratory experiment. The example chosen for this first attempt is the appearance of a nonspreading quantum-like oscillating wave packet in a compressible fluid (e.g. a plasma) subjected to an attractive harmonic oscillator potential.

## 2. Theoretical Background

Let us sum up the results described in more detail in Ref. 2. We consider a classical macroscopic compressible fluid described by the Euler and the continuity equations:

$$\left(\frac{\partial}{\partial t} + V \cdot \nabla\right)V = -\nabla\phi, \quad (1)$$

$$\frac{\partial\rho}{\partial t} + \text{div}(\rho V) = 0, \quad (2)$$

where  $\phi$  is an exterior scalar potential. We assume as a first step that the pressure term is negligible and that the fluid motion is potential, i.e.

$$V = \nabla S. \quad (3)$$

We now assume that we apply to the fluid (using density measurements and a retroaction loop) a varying force which is a function of the fluid density in real time, namely, a “quantum-like” force  $F_Q$  deriving from the potential

$$Q = -2\mathcal{D}^2 \frac{\Delta\sqrt{\rho}}{\sqrt{\rho}}. \quad (4)$$

This potential is a generalization of the standard quantum potential,<sup>4</sup> since here the constant  $\mathcal{D}$  can have any value, while in standard quantum mechanics it is restricted to the only value  $\mathcal{D} = \hbar/2m$ . As recalled in what follows, this generalization still allows to recover a Schrödinger-like equation.

The Euler and continuity system becomes

$$\left(\frac{\partial}{\partial t} + V \cdot \nabla\right)V = -\nabla\left(\phi - 2\mathcal{D}^2 \frac{\Delta\sqrt{\rho}}{\sqrt{\rho}}\right), \quad (5)$$

$$\frac{\partial\rho}{\partial t} + \text{div}(\rho V) = 0. \quad (6)$$

The system of Eqs. (5) and (6) can then be integrated under the form of a generalized Schrödinger equation.

Indeed, Eq. (5) takes the successive forms

$$\frac{\partial}{\partial t}(\nabla S) + \frac{1}{2}\nabla(\nabla S)^2 + \nabla\left(\phi - 2\mathcal{D}^2\frac{\Delta\sqrt{\rho}}{\sqrt{\rho}}\right) = 0, \quad (7)$$

$$\nabla\left(\frac{\partial S}{\partial t} + \frac{1}{2}(\nabla S)^2 + \phi - 2\mathcal{D}^2\frac{\Delta\sqrt{\rho}}{\sqrt{\rho}}\right) = 0, \quad (8)$$

which can be integrated as

$$\frac{\partial S}{\partial t} + \frac{1}{2}(\nabla S)^2 + \phi + K - 2\mathcal{D}^2\frac{\Delta\sqrt{\rho}}{\sqrt{\rho}} = 0, \quad (9)$$

where  $K$  is a constant that can be renormalized by a redefinition of the potential energy  $\phi$ . Let us now combine this equation with the continuity equation as follows:

$$\left[ -\frac{1}{2}\sqrt{\rho}\left(\frac{\partial S}{\partial t} + \frac{1}{2}(\nabla S)^2 + \phi - 2\mathcal{D}^2\frac{\Delta\sqrt{\rho}}{\sqrt{\rho}}\right) + i\frac{\mathcal{D}}{2\sqrt{\rho}}\left(\frac{\partial\rho}{\partial t} + \text{div}(\rho\nabla S)\right) \right] e^{iS/2\mathcal{D}} = 0. \quad (10)$$

Finally we set

$$\psi = \sqrt{\rho} \times e^{iS/2\mathcal{D}}, \quad (11)$$

and Eq. (10) is strictly identical to the following generalized Schrödinger equation

$$\mathcal{D}^2\Delta\psi + i\mathcal{D}\frac{\partial}{\partial t}\psi - \frac{\phi}{2}\psi = 0, \quad (12)$$

as can be checked by replacing in it  $\psi$  by its expression (11). Recall that such an equation has also been directly obtained, in terms of a density of probability instead of a density of matter, as the integral of the equations of geodesics in a non-differentiable space-time.<sup>5,6</sup> Given the linearity of the equation obtained, one can normalize the modulus of  $\psi$  by replacing the matter density  $\rho$  by a probability density  $P = \rho/M$ , where  $M$  is the total mass of the fluid in the volume considered: this will be equivalent.

The solutions  $\psi = |\psi| \times \exp(i\theta)$  of this equation directly provide the density and the velocity field of the fluid at every point, namely

$$V = 2\mathcal{D}\nabla\theta, \quad \rho = M|\psi|^2. \quad (13)$$

Its imaginary part and its real part amount, respectively, to the continuity equation, and to the energy equation that writes:

$$E = -\frac{\partial S}{\partial t} = \frac{1}{2}V^2 + \phi - 2\mathcal{D}^2\frac{\Delta\sqrt{\rho}}{\sqrt{\rho}}. \quad (14)$$

The above transformation from the fluid mechanics-like equations to the Schrödinger-type equation is similar to a Madelung transformation,<sup>7</sup> but it is here performed in the reversed way and generalized to a constant different from  $\hbar/2m$ .<sup>2</sup>

It could be therefore possible by this method to simulate a “Schrödinger system,” e.g. a partly quantum-like superfluid system coming under two of the axioms of quantum mechanics, namely, (i) it is described by a wave function  $\psi$  which is solution of a Schrödinger-type equation and (ii) such that  $\rho \propto |\psi|^2$ .

### 3. Application to the Oscillating Wave Packet

As an example of application and as a preparation for a laboratory experiment, let us consider the simplified case of one-dimensional fluid motion in an external harmonic oscillator potential  $\phi = (1/2)\omega^2 x^2$ . This system is described by the two following equations:

$$\frac{\partial V}{\partial t} = -V \frac{\partial V}{\partial x} - \omega^2 x + 2\mathcal{D}^2 \frac{\partial}{\partial x} \left( \frac{\partial^2 \sqrt{\rho} / \partial x^2}{\sqrt{\rho}} \right), \quad (15)$$

$$\frac{\partial \ln \rho}{\partial t} = - \frac{\partial V}{\partial x} - V \frac{\partial \ln \rho}{\partial x}. \quad (16)$$

Here we have written the continuity equation in terms of  $\ln \rho$  instead of its usual expression in terms of  $\rho$ . This form of the continuity equation which be useful in the numerical simulations that follow. These two equations are equivalent to the one-dimensional generalized Schrödinger equation:

$$\mathcal{D}^2 \frac{\partial^2 \psi}{\partial x^2} + i\mathcal{D} \frac{\partial \psi}{\partial t} - \frac{1}{4} \omega^2 x^2 \psi = 0. \quad (17)$$

It is well-known that it is possible to find a solution of this equation in the form of a wave packet whose center of gravity oscillates with the period of the classical motion and which shows no spreading with time.<sup>8-10</sup> Assuming that the maximal amount by which the center of gravity is displaced is  $a$ , the wave function  $\psi = \sqrt{P} \times e^{iS/2\mathcal{D}}$  reads in this case

$$\psi = \left( \frac{\omega}{2\pi\mathcal{D}} \right)^{\frac{1}{4}} e^{-\frac{i\omega}{4\mathcal{D}}(x-a \cos \omega t)^2} \times e^{-i\left(\frac{1}{2}\omega t + \frac{\omega}{2\mathcal{D}} a x \sin \omega t - \frac{\omega}{8\mathcal{D}} a^2 \sin 2\omega t\right)}. \quad (18)$$

Therefore the probability density reads

$$P = |\psi|^2 = \sqrt{\frac{\omega}{2\pi\mathcal{D}}} e^{-\frac{\omega}{2\mathcal{D}}(x-a \cos \omega t)^2}, \quad (19)$$

and the action  $S = 2\mathcal{D}\theta$

$$S = -\mathcal{D}\omega t - a\omega x \sin \omega t + \frac{1}{4} a^2 \omega \sin 2\omega t. \quad (20)$$

It is easily generalized to a three-dimensional wave packet oscillating in one direction. In this case the probability reads

$$P = \sqrt{\frac{\omega}{2\pi\mathcal{D}}} e^{-\frac{\omega}{2\mathcal{D}}[(x-a\cos\omega t)^2+y^2+z^2]}. \quad (21)$$

In what follows we shall consider only the  $x$  dependence.

This is an interesting case for a test of a genuine quantum-like behavior, since it involves a nonvanishing phase in an essential way although this is a one-dimensional system. The velocity field is given by

$$V = -a\omega \sin \omega t. \quad (22)$$

The quantum potential reads

$$Q(x, t) = \mathcal{D}\omega - \frac{1}{2}\omega^2(x - a \cos \omega t)^2, \quad (23)$$

and the quantum force,

$$F_Q(x, t) = -\frac{\partial Q}{\partial x} = \omega^2(x - a \cos \omega t). \quad (24)$$

Therefore the energy  $E = -\partial S/\partial t$ , which is here a “field” depending on the space and time coordinates, takes the form

$$E(x, t) = \frac{1}{2}V^2 + \phi + Q = \mathcal{D}\omega + a\omega^2 x \cos \omega t - \frac{1}{2}a^2\omega^2 \cos(2\omega t). \quad (25)$$

When it is applied to the center of the wave packet  $x = a \cos \omega t$ , this expression becomes

$$E_c = \mathcal{D}\omega + \frac{1}{2}a^2\omega^2. \quad (26)$$

We recognize in the second term, as expected, the energy of a classical pendulum. Concerning the first term, since standard quantum mechanics corresponds to the particular choice  $\mathcal{D} = \hbar/2m$  (here with  $m = 1$ ), the term  $\mathcal{D}\omega$  is the generalization of the vacuum energy for an harmonic oscillator,  $E_{\text{vac}} = (1/2)\hbar\omega$ .

Therefore we verify that the application of a quantum potential on the fluid has given to it some new properties of a quantum-like nature, such as a zero-point energy and the conservation of the shape of the wave packet.

#### 4. Proposed Laboratory Experiment

In order to prepare a real laboratory experiment aiming at achieving such a new macroscopic quantum-like (super)fluid, we shall now present the result of numerical simulations of such an experiment. To this purpose these simulations are not based on the Schrödinger form of the equations, but instead on the classical Euler + continuity equations and on the application by feedback of a generalized quantum-like force.

The suggested experiment consists of:

- (i) measuring with detectors the density at regular time interval  $\{t_n\}$  on a grid at positions  $\{x_j\}$ ;
- (ii) computing from these measurements the quantum force  $(F_Q)_n = 2\mathcal{D}^2\nabla(\Delta\sqrt{\rho_n}/\sqrt{\rho_n})$  at each time  $t_n$ ;
- (iii) applying the new value of the force to the fluid at each time  $t_n$ , therefore simulating by such a feedback the presence of a quantum-like potential.

The advantage of such a proposal is that one is no longer constrained by the standard quantum value  $\mathcal{D} = \hbar/2m$  that fixes the amplitude of the quantum force, and that one can therefore give to it a macroscopic value, vary it, study its transition to zero (quantum to classical transition), etc.

## 5. Iterative Fitting Simulation

In this first simulation, we assume that the quantum force (which is a third derivative of the density) is not computed directly from the values of the density, but from a polynomial fit of the distribution of  $\ln \rho$ . In the special case considered here (the oscillating wave packet), we use a Gaussian fit of the density distribution (i.e. a second-order polynomial fit to  $\ln \rho$ ), so that we need to know only the mean and dispersion. More generally, one can decompose the distribution of  $\ln \rho(x)$  into its successive moments. Therefore the density is written as

$$\rho_n(x) \propto \exp\left[-\frac{1}{2}\left(\frac{x - \bar{x}_n}{\sigma_n}\right)^2\right], \quad (27)$$

so that, once the mean and dispersion  $\bar{x}_n$  and  $\sigma_n$  at time  $t_n$  are computed, the quantum force to be applied at each step ( $n$ ) writes:

$$(F_Q)_n(x) = \frac{\mathcal{D}^2(x - \bar{x}_n)}{\sigma_n^4}. \quad (28)$$

### 5.1. Numerical simulation

Our numerical simulation is performed by a simple Mathematica program which reproduces the steps of the real experiment, namely, at each time step  $t_n$ :

- (i) We compute the mean and the dispersion of positions  $x$  according to the density distribution:

$$\bar{x} = \frac{\sum_j \rho(x_j)x_j}{\sum_j \rho(x_j)}, \quad (29)$$

$$\sigma^2 = \frac{\sum_j \rho(x_j)(x_j - \bar{x})^2}{\sum_j \rho(x_j)}. \quad (30)$$

(ii) The force  $F_Q$  to be added then writes in terms of these quantities

$$(F_Q)_n(x) = \frac{\mathcal{D}^2(x - \bar{x}_n)}{\sigma_n^4 \delta x^3}, \quad (31)$$

where  $\delta x$  is the grid interval and intervenes here because we use finite differences.

(iii) We compute the logarithm of the density  $\ln \rho$  and the velocity  $V$  at next time step  $t_{n+1}$  by transforming Eqs. (15) and (16) into centered finite-difference equations (forward time centered space, FTCS scheme) using the Lax–Friedrichs method,<sup>11</sup> namely,

$$\begin{aligned} \ln \rho_j^{n+1} = & \frac{\ln \rho_{j+1}^n + \ln \rho_{j-1}^n}{2} - \frac{\delta t}{2\delta x} \{(V_{j+1}^n - V_{j-1}^n) \\ & + V_j^n (\ln \rho_{j+1}^n - \ln \rho_{j-1}^n)\}, \end{aligned} \quad (32)$$

$$V_j^{n+1} = \frac{V_{j+1}^n + V_{j-1}^n}{2} + \delta t \left( -V_j^n \frac{V_{j+1}^n - V_{j-1}^n}{2\delta x} + F_j^n + (F_Q)_j^n \right). \quad (33)$$

The lower index ( $j$ ) is for space  $x$  and the upper one ( $n$ ) is for time  $t$ ;  $\delta t$  is the time step and  $F(x) = -\omega^2 x$  is the external harmonic oscillator force. In the above Lax method, the terms  $\ln \rho_j^n$  and  $V_j^n$  are replaced by their space average, which has the advantage to stabilize the FTCS scheme.

The initial conditions are given by the density distribution Eq. (19) for  $t = 0$ .

Although this is a simple scheme (we have not attempted at this stage to better control numerical error diffusion), it has given very encouraging results, since it has reproduced on several periods the expected motion of the quantum oscillating wave packet (see Fig. 1).

## 5.2. Perturbation of initial conditions

One of the possible shortcomings in the passage from the simulation to a real experiment may come from fluctuations in the initial conditions. Indeed, in the previous simulations, we have taken as initial density distribution that of the exact quantum wave packet. In order to be closer to a real experimental situation, we have therefore performed a new simulation similar to that of Sec. 5.1, but with an initial density distribution that is perturbed with respect to the Gaussian solution Eq. (19): We have multiplied its values  $\rho(x_j)$  at each point  $\{x_j\}$  of the space grid by  $e^{f\alpha_j}$ , where  $\alpha_j$  is random in the interval  $[0, 1]$ . In other words, we have added random values  $f\alpha_j$  to the initial values of  $\ln \rho_j^0$ , i.e.

$$\rho_0(x, 0) = \sqrt{\frac{\omega}{2\pi\mathcal{D}}} \times e^{f\alpha(x) - (x-x_0)^2/2\sigma_0^2}. \quad (34)$$

A typical resulting initial density distribution is given in Fig. 2 for a fluctuation amplitude  $f = 1$  (equivalent to  $\sqrt{2}\sigma_0$  according to the above equation), followed by

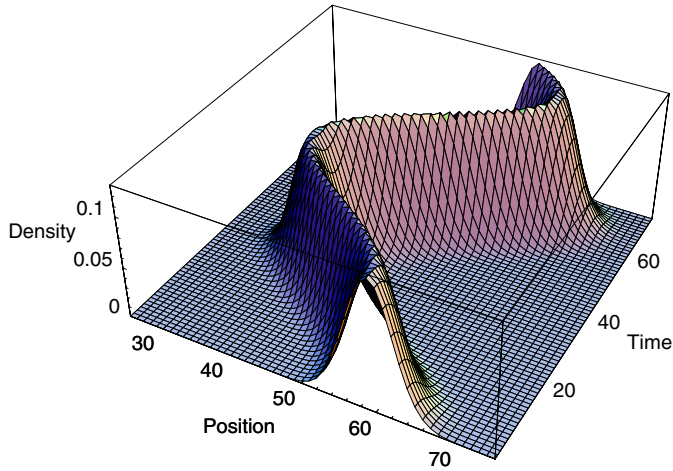


Fig. 1. (Color online) Result of the numerical integration of a Euler + continuity one-dimensional system with generalized quantum potential for the oscillating wave packet in an harmonic oscillator field. The quantum force applied on the fluid is calculated from a Gaussian fit of the density distribution. The figure gives the density distribution obtained in function of position (space grid from 25 to 75) and time (time steps from 1 to 75, i.e. 1.2 period).

the distributions obtained on a full period (sub-figures 1–12) after application of the generalized quantum force.

Once again the result obtained is very encouraging as concerns the possibility of performing a real laboratory experiment, since, despite the initial deformation, the wave packet remains stable during several periods. Moreover, not only the mean and dispersion of the evolving density distribution remain close to the ones expected for the quantum wave packet, but, as can be seen in Fig. 2, the initial perturbations have even been smoothed out during the feedback process.

### 5.3. More general account of uncertainties

#### 5.3.1. Density fluctuations

This encouraging result leads us to attempt a numerical simulation under far more difficult conditions: In order to simulate the various uncertainties and errors that may occur in a real experiment, in particular as concerns the density measurement, the application of the force and physical effects not accounted in the simulation such as vorticity (when going to more than one dimension), etc. we now add a fluctuation at each step of the retroactive loop (for the effect of pressure, see below). Namely, at each time step  $t_n$ , we multiply the density  $\rho(x_j)$  at each point  $\{x_j\}$  of the space grid by  $e^{f\alpha_j}$ , where  $\alpha_j$  is random in the interval  $[0, 1]$ . In other words, Eq. (35) becomes

$$\begin{aligned} \ln \rho_j^{n+1} = & \frac{\ln \rho_{j+1}^n + \ln \rho_{j-1}^n}{2} - \frac{\delta t}{2\delta x} \{(V_{j+1}^n - V_{j-1}^n) \\ & + V_j^n (\ln \rho_{j+1}^n - \ln \rho_{j-1}^n)\} + f_d \alpha_j. \end{aligned} \quad (35)$$



As can be seen in Fig. 3, despite the large errors added, the numerical simulation shows an oscillating wave packet with large fluctuations which nevertheless keeps its coherence. In particular, it keeps the values of the mean and dispersion (to about 5 percent) expected for the quantum solution during the whole simulation (which ends because of numerical errors after a full period for  $f_d = 1/2$  and half a period for  $f_d = 1$ ).

### 5.3.2. Velocity fluctuations

Another way to put the stability of the simulation to the test consists in adding fluctuations directly on the velocity field instead of the density. This test is more

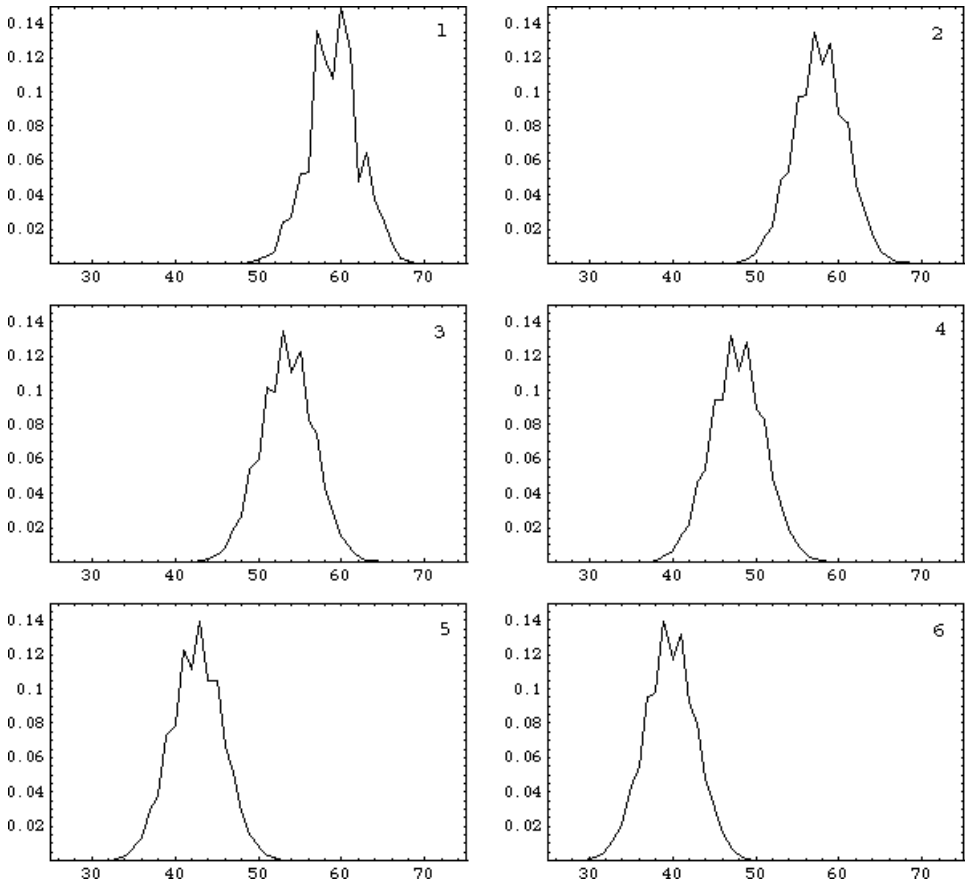


Fig. 2. Result of the numerical integration of a Euler + continuity one-dimensional system with added quantum potential, in the case of an oscillating wave packet. The conditions are the same as in Fig. 1, except for the addition of a perturbation on the initial density distribution (left top figure). The quantum force applied on the fluid is calculated from a Gaussian fit of the density distribution. The successive figures give the density distribution obtained in function of position (space grid from 25 to 75) and time (64 time steps corresponding to one period, among which 12 of them, equally distributed, are shown).

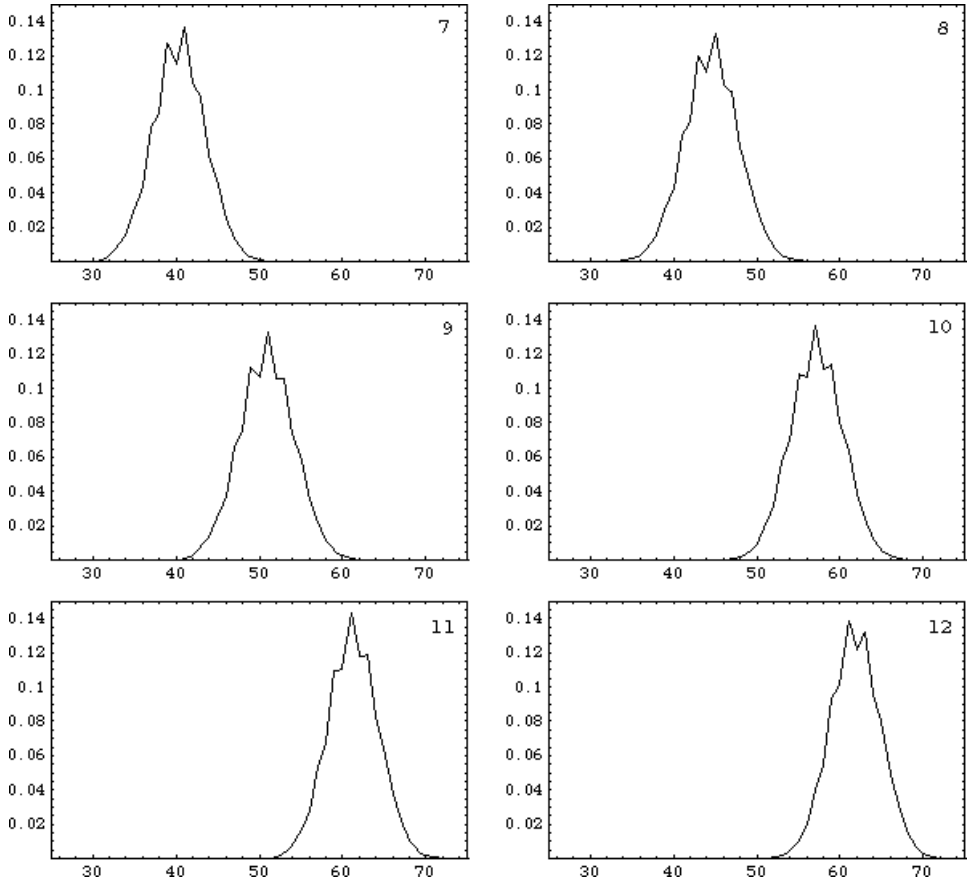


Fig. 2. (Continued)

adapted to anticipating the possible effects of vorticity and turbulence, owing to the fact that the velocity is to the square in the energy equation. Once again we add a fluctuation at each time step of the process, similar to a self-sustained fluctuation of the type provided by turbulence. Here the fluctuation added is chosen to be Gaussian.

Therefore Eq. (33) becomes:

$$V_j^{n+1} = \frac{V_{j+1}^n + V_{j-1}^n}{2} + \delta t \left( -V_j^n \frac{V_{j+1}^n - V_{j-1}^n}{2\delta x} + F_j^n + (F_Q)_j^n \right) + f_v \xi, \quad (36)$$

where  $\xi$  is a stochastic variable with a normalized and centered Gaussian distribution.

An example of the result obtained is given in Fig. 4 (for  $f_v = 0.2$ ). Clearly, the effect of velocity perturbations is stronger than that of density perturbations (as expected).

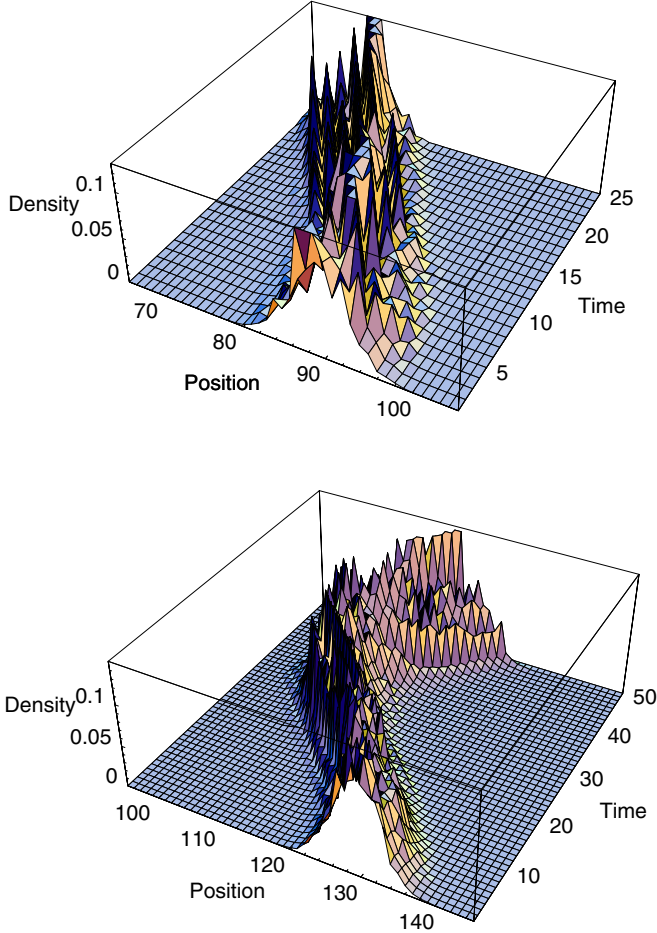


Fig. 3. (Color online) Result of the numerical integration of a Euler + continuity one-dimensional system with added generalized quantum potential, in the case of an oscillating wave packet. The conditions are the same as in Fig. 1, except for the addition of a perturbation  $e^{f\alpha(x)}$  on the density distribution at each time step of the simulation. The fluctuation  $\alpha(x)$  is simulated by a stochastic variable which is random in the interval  $[0, 1]$ . The quantum force applied on the fluid is calculated from a Gaussian fit of the density distribution. The figures give the density distribution obtained in function of position and time. The top figure corresponds to a fluctuation amplitude  $f = 1$  (the simulation ended after one half period due to numerical errors). The down figure corresponds to a fluctuation amplitude  $f = 0.5$ . In this case the simulation was continued on nearly a full period before ending due to numerical errors.

However, we see that the wave packet, although it loses its Gaussian shape and becomes highly fluctuating, keeps its mean motion and its dispersion during all the simulation (which ends here after about half a period due to numerical errors). This is an encouraging result which allows one to expect that, in a real experiment, small deviations from potential motion and other velocity fluctuations, although they would certainly perturb the experimental process, would not prevent the main researched structure to appear, i.e. that of an oscillatory nonspreading wave packet.

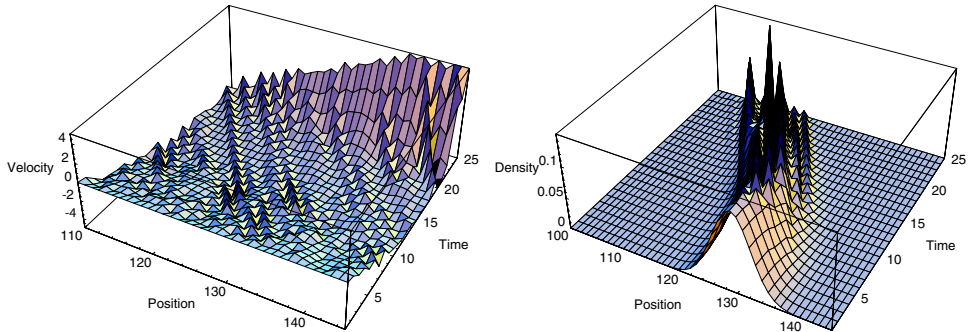


Fig. 4. (Color online) Result of the numerical integration of a Euler + continuity one-dimensional system with added generalized quantum potential, in the case of an oscillating wave packet. The conditions are the same as in Fig. 1, except for the addition of a Gaussian perturbation on the velocity distribution at each time step of the simulation, with here  $f_v = 0.2$  (see text). The quantum force applied on the fluid is calculated from a Gaussian fit of the density distribution. The left figure gives the velocity field and the right figure the density distribution obtained in function of position and time. The simulation ends after about half a period.

#### 5.4. Account of pressure

The addition of a pressure term in the initial Euler equation still allows one to obtain a Schrödinger-like equation in the general case when  $\nabla p/\rho$  is a gradient, i.e.  $\nabla p/\rho = \nabla w$ . This is the case of an isentropic fluid and, more generally, of every cases when there is an univocal link between pressure and density, e.g. a state equation.<sup>12</sup> The Euler equation with quantum potential and external potential reads

$$\left(\frac{\partial}{\partial t} + V \cdot \nabla\right)V = -\nabla\left(\phi + w - 2\mathcal{D}^2\frac{\Delta\sqrt{\rho}}{\sqrt{\rho}}\right), \quad (37)$$

and it can therefore, in combination with the continuity equation, be integrated in terms of a Schrödinger-like equation,

$$\mathcal{D}^2\Delta\psi + i\mathcal{D}\frac{\partial}{\partial t}\psi - \frac{\phi + w}{2}\psi = 0. \quad (38)$$

Now the pressure term needs to be specified through a state equation, which can be chosen as taking the general form  $p = k_p\rho^\gamma$ . The special case  $\gamma = 1$  can be recovered and its amplitude established by taking the acoustic limit  $p = p_0 + p'$ ,  $\rho = \rho_0 + \rho'$  and  $p' = c_s^2\rho'$ , where  $c_s$  is the sound velocity in the fluid. Therefore one obtains a linear relation  $p = a + c_s^2\rho$ , so that the pressure term in the Euler equation finally reads  $\nabla p/\rho = k_p\nabla\ln\rho$ , while  $w = k_p\ln\rho = k_p\ln|\psi|^2$ , with  $k_p = c_s^2$ . This means that the integrated equation is now a nonlinear Schrödinger equation,

$$\mathcal{D}^2\Delta\psi + i\mathcal{D}\frac{\partial}{\partial t}\psi - k_p\ln|\psi|\psi = \frac{1}{2}\phi\psi. \quad (39)$$

In the highly compressible case the dominant pressure term is rather  $p \propto \rho^2$  and the  $\ln|\psi|$  term is replaced by  $|\psi|^2$  in the nonlinear Schrödinger equation (see e.g. Ref. 13).

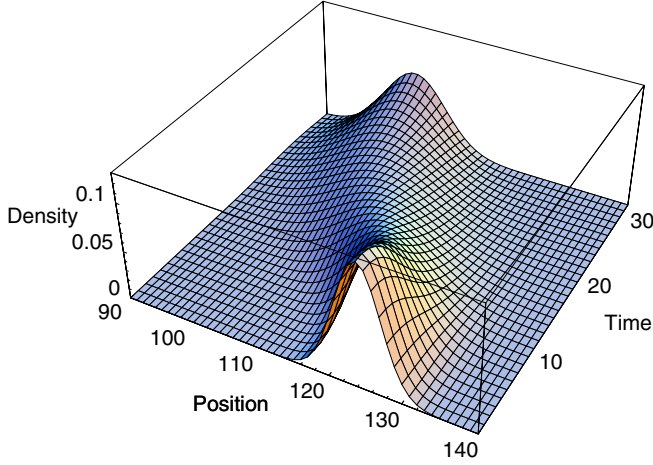


Fig. 5. (Color online) Result of the numerical integration of a Euler and continuity one-dimensional system of equations with added generalized quantum potential and account of a pressure term, for the oscillating wave packet. The quantum force applied on the fluid is calculated from a Gaussian fit of the density distribution. The figure gives the probability density in function of position (space grid from 90 to 140) and time (time steps from 1 to 32). In this simulation (near half a period), the amplitude of the pressure term is  $k_p = 5$ .

The numerical integration is now performed by generalizing Eq. (33) as

$$V_j^{n+1} = \frac{V_{j+1}^n + V_{j-1}^n}{2} + \delta t \left( -V_j^n \frac{V_{j+1}^n - V_{j-1}^n}{2\delta x} + F_j^n + (F_Q)_j^n - k_p \frac{\ln \rho_{j+1}^n - \ln \rho_{j-1}^n}{2\delta x} \right). \quad (40)$$

The result is given in Figs. 5 and 6 for two different values of the pressure amplitude  $k_p$ . One finds that the addition of pressure leads to a small oscillation of the width of the wave packet, but that its main quantum fluid-like features are preserved, since it nearly recovers its shape after half a period.

## 6. Full Finite Difference Simulation

The success of this first simple simulation leads us to attempt a more direct feedback in which the quantum force is computed by finite differences from the values of the density itself (while in the previous simulation we used an intermediate polynomial fit from which the force was analytically derived).

To this purpose, we use a form of the generalized quantum potential and of the generalized quantum force according to which they can be expressed in terms of only  $\nabla \ln P$  (or equivalently  $\nabla \ln \rho$ ). Setting

$$H = \nabla \ln P, \quad (41)$$

we find:

$$Q = -\mathcal{D}^2 \left( \nabla \cdot H + \frac{1}{2} H^2 \right), \quad (42)$$

$$F_Q = -\nabla Q = \mathcal{D}^2 [\Delta H + (H \cdot \nabla) H]. \quad (43)$$

In one dimension it reads

$$F_Q = \mathcal{D}^2 \left( \frac{\partial^3 \ln P}{\partial x^3} + \frac{\partial^2 \ln P}{\partial x^2} \frac{\partial \ln P}{\partial x} \right). \quad (44)$$

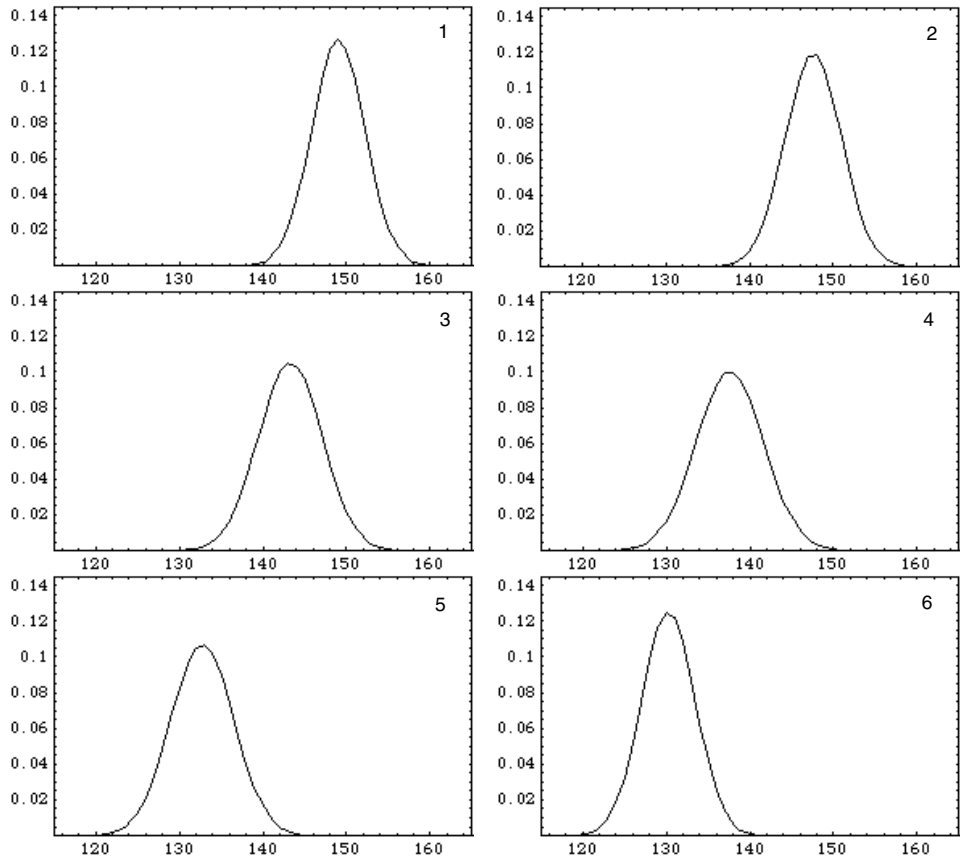


Fig. 6. Result of the numerical integration of a Euler and continuity one-dimensional system of equations with added generalized quantum potential and account of a pressure term, for the oscillating wave packet. The quantum force applied on the fluid is calculated from a Gaussian fit of the density distribution. The figure gives the density distribution in function of the position (space grid from 120 to 160), for 12 equal time steps which cover a full period. In this simulation, the amplitude of the pressure term is  $k_p = 1$ . One sees that the effect of pressure amounts to a small oscillation of the width and height of the wave packet, which nearly recovers its shape after half a period.

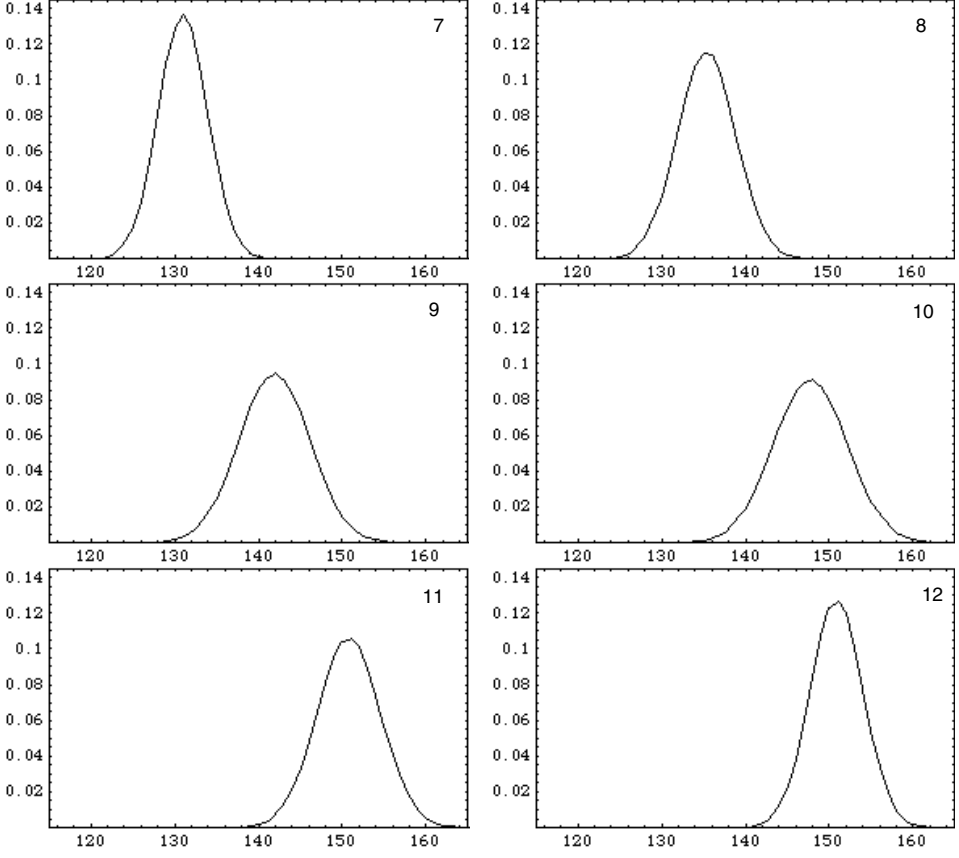


Fig. 6. (Continued)

The numerical integration proceeds following the same lines as in the previous simulation, except for the first steps aiming at computing  $F_Q$ , which are replaced by a finite difference calculation according to Eq. (43). Such a way to compute the force  $F_Q$  to be applied on the fluid is therefore directly similar to its calculation in a real laboratory experiment from digitalized measurements of the density by a grid of detectors. Namely, we calculate successively, for all values of the position index  $j$ ,

$$H_j^n = \frac{\ln \rho_{j+1}^n - \ln \rho_{j-1}^n}{2\delta x}, \quad (45)$$

then similar relations for positions  $x_{j-1}$ ,  $x_{j+1}$ ,  $x_{j-2}$  and  $x_{j+2}$ , then

$$Q_{j-1}^n = -\mathcal{D}^2 \left\{ \frac{H_j^n - H_{j-2}^n}{2\delta x} + \frac{1}{2} (H_{j-1}^n)^2 \right\}, \quad (46)$$

then a similar relation for  $Q(x_{j+1}, t_n)$  and finally

$$(F_Q)_j^n = \frac{Q_{j-1}^n - Q_{j+1}^n}{2\delta x}. \quad (47)$$

The calculation of  $\ln \rho$  (from the continuity equation) and of  $V$  (from the Euler equation) are the same as previously.

We have also attempted to use other more precise formulas for the calculation of the first, second and third order derivatives in the expression of  $F_Q$ , namely, expressions valid up to order  $O(\delta x^4)$  (see Appendix A),

$$f' = \frac{-f_2 + 8f_1 - 8f_{-1} + f_{-2}}{12\delta x}, \quad (48)$$

$$f'' = \frac{-f_2 + 16f_1 - 30f_0 + 16f_{-1} - f_{-2}}{12\delta x^2}, \quad (49)$$

$$f''' = \frac{-f_3 + 8f_2 - 13f_1 + 13f_{-1} - 8f_{-2} + f_{-3}}{8\delta x^3}, \quad (50)$$

where the indices are here the differences with  $j$  and where  $x_j = 0$ . This has led to essentially the same result.

Despite, once again, the roughness of the chosen integration method, the result obtained is satisfactory, since the motion of a quantum nonspreading oscillating wave packet has been reproduced on up to a full period before divergence due to the effect of computing errors (Fig. 7). We stress once again the fact that this result has been obtained without using the Schrödinger equation, but instead an apparently “classical” hydrodynamic Euler/continuity system with an externally applied generalized quantum potential.

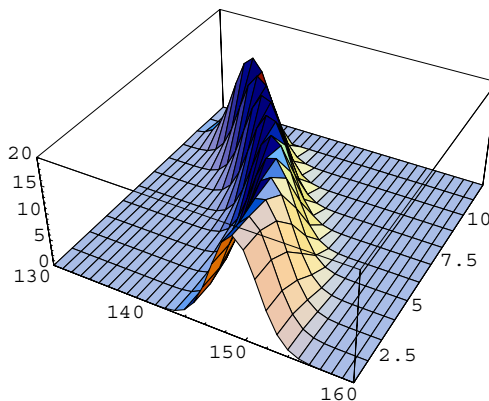


Fig. 7. (Color online) Result of the numerical integration of a Euler + continuity one-dimensional system with generalized quantum potential for the oscillating wave packet in an harmonic oscillator field. The quantum force applied on the fluid is directly calculated from the values of the density by finite differences. The density distribution obtained in function of position (space grid from 130 to 160) has been followed on about 0.4 period before divergence due to the effect of computing errors).



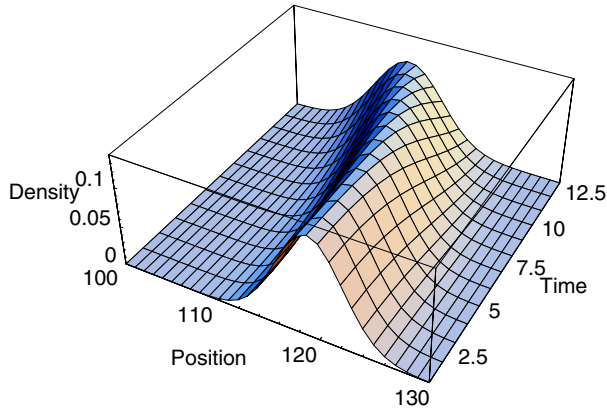


Fig. 8. (Color online) Result of the numerical integration of a Euler + continuity one-dimensional system with generalized quantum potential for the oscillating wave packet in an harmonic oscillator field and account of pressure (1/4 of period before stop due to computing errors). The quantum force applied on the fluid is here directly calculated from the values of the density by finite differences. The figure gives the probability density in function of space (grid from 100 to 130) and time (time steps from 1 to 13). A pressure term has been added ( $k_p = 1$ , whose effect is a slight oscillatory deformation of the wave packet).

Adding a pressure term yields a similar result (i.e. reproduction of the motion of the wave packet on about one period before divergence due to the effect of computing errors) which confirms the result obtained with the Gauss fitting method, namely, a partial oscillating spreading of the wave packet (Fig. 8).

## 7. Feasibility of the Proposed Experiment

The proposed experiment is based on a feedback loop involving measurement of the density field of a fluid, computing of the macroquantum potential and force in function of the density measurement results, then simulation of the macroquantum force though application of a classical field having the expected form.

A full description of such an experiment is outside the scope of this paper. However, we give in the present section some elements about its feasibility, in the case of an application to a plasma.

Concerning the second step of the loop (computing), we note that the numerical simulations presented in this paper are by nature discretized, so that they closely apply to the type of experiment considered. Finite difference formulas allowing to calculate first and second derivatives with a  $O[\varepsilon^4]$  precision are given in Appendix A. Let us give some elements about the two others steps (detectors and actuators) indicating that such an experiment should indeed be feasible with today's technology.

### 7.1. Plasma density measurements

Several classical methods are available to probe the density of a plasma, in particular its electronic density. Among them nonperturbative methods relying on the

launching of waves of electromagnetic radiation such as interferometry and reflectometry are suitable in particular for inhomogeneous plasmas and are easy to handle.<sup>14</sup> We shall focus here on the reflectometry technique. Its principle is easy to describe: An external electromagnetic wave is launched at a given frequency  $f_0$  such that somewhere within the plasma the condition  $f_0 = f_p$  is met, where

$$2\pi f_p = \left[ \frac{n(x) \cdot e^2}{m_e \cdot \epsilon_0} \right]^{1/2} \quad (51)$$

is the plasma frequency and  $n(x)$  the local electronic density.

This equality (51) defines the location  $x = x_c$  of the cut-off layer. For an isotropic (nonmagnetized plasma) the dispersion relation for a (transverse) electromagnetic wave reads:

$$\omega^2 = \omega_p^2(x) + 3k^2 V_{\text{the}}^2 + k^2 c^2. \quad (52)$$

Neglecting the thermal velocity  $V_{\text{the}}$  (with  $V_{\text{the}}^2 = k_B T_e / m_e$ ) one thus obtains  $k = 0$  for  $\omega = \omega_p$  (or  $f = f_p$  as above): The plasma acts as a perfect mirror at the cut-off layer. The experiment then consists in launching with a suitable generator a wave of a given frequency. By sweeping the frequency one can obtain the whole density profile.

In a classical reflectometer the variation of the wave phase is measured along the wave path toward and back from the cut-off layer. One thus gets:

$$\Delta\phi(f) = 2 \int_0^{x_c} k(x, f) dx, \quad (53)$$

$k$  being the wave number as given by the dispersion relation (52). This wave number  $k = k(x)$  is a function of  $x$  since it depends on  $n(x)$ .

An Abel inversion is necessary to get the  $x_c$  position (this sets conditions on the shape of the density profile) as:

$$x_c(f_0) = \frac{c}{2\pi^2} \int_0^{f_0} \frac{d\Delta\phi(f)/df}{(f_0^2 - f^2)^{1/2}} df. \quad (54)$$

Of course this measure supposes that the density profile remains constant during the measurement time. To reduce this time one often uses a pulse electromagnetic wave and compute the time of flight between the emission and the reception of the signal.

In case of a pulse, the time of flight  $t_0$  is given by  $t_0 = \int (dx/v_g(x))$ , where  $v_g(x)$  is the group velocity, so that one obtains:

$$t_0(f) = 2 \int_0^{x_c} \frac{dx}{v_g(x)} = \frac{2}{c} \int_0^{x_c} \left( \frac{1}{1 - (f_p(x)/f)^2} \right)^{1/2} dx. \quad (55)$$

The time of flight can be connected with the phase as follows:

$$t_0(f) = \frac{d}{df} \Delta\phi(f). \quad (56)$$

Therefore one can write also  $x_c(f) = (c/\pi) \int_0^f t_0(f') / (f^2 - f'^2)^{1/2} df'$ . By recording the time of flight, one thus recovers the density profile. Such measurements are currently undertaken in plasma experiments with high resolutions adapted to the here proposed device.

### 7.2. Application of a force on a plasma

Once the density  $n(x)$  has been measured with the required resolution, the macro-quantum force can be computed as  $F = 2\mathcal{D}^2 \nabla(\Delta \sqrt{n} / \sqrt{n})$ . Then we simulate its profile by a classical force. The application of a given force profile on a plasma is an easy task thanks to the fact it is charged and compressible. The plasma can therefore be sensible to various type of forces: Mostly pressure forces  $p$  and electromagnetic forces  $(E, B)$ .

Concerning the use of pressure, one can launch acoustic waves in the plasma. Since for dilute plasmas it is close to a perfect gas,  $p$  is proportional to  $nT$ , so that thermal effects could also be used to simulate the macroquantum force.

In the case of electromagnetic forces one can easily modulate the electric field  $E$  profile and/or the magnetic field  $B$  profile to give them the required macroquantum-like shape. The induced electromagnetic fields (polarization effects) due to the external applied fields will be taken into account in the calculation of the full applied force.

## 8. Discussion and Conclusion

These preliminary simulations were intended to yield a first validation of the concept of a new kind of quantum-like macroscopic experiments based on the application to a classical system of a generalized quantum-type force through a retroaction loop.<sup>1,2</sup> They have given a positive results, since the expected quantum-type stable structure (here a nonspreading oscillating wave packet, or, in the case of pressure, an oscillatory wave packet with a slightly oscillating width) has been obtained during a reasonably long time of integration. These results, obtained by two simple integration methods, are very encouraging since they give the hope that a real laboratory experiment should be possible to achieve.

In the hydrodynamic case considered in this work, possible shortcomings are to be considered in a real experiment, such as the effects of finite compressibility, of vorticity, of viscosity at small scales, of density detector uncertainties, of the minimal time interval needed to perform the loop for the calculation, then the uncertainties linked to application of the quantum force, etc.

We have attempted here to have a first account of these uncertainties by taking a pressure term into account, by adding large random fluctuations in the initial conditions, then by adding large fluctuations at each time steps of the simulation, on the density distribution as well as on the velocity field. The results obtained were again encouraging, since, despite the pressure term and the large fluctuations, the overall coherence of the wave packet and its period were preserved.

Concerning the question of vorticity, it is too wide to be discussed in detail in the present paper, which is devoted to the description of a specific experiment restrained to a potential fluid. It will be the subject of forthcoming works. Let us simply remark that the application of the quantum potential to a potential fluid is not expected to introduce vorticity. On the contrary, we hope that it will in some situations increase the irrotational part of a fluid. The example of the transition from a classical vortex to a quantum-like vortex<sup>15</sup> is enlightening in this regard. Indeed, the classical vortex is potential in its outer region and rotational in the inner region which rotates like a solid body, while the quantum vortex (see e.g. Ref. 16) is everywhere potential. We therefore expect that, in the new experiment, the application of a quantum-type potential will increase the size of the outer irrotational zone. Moreover, one can show<sup>2</sup> that the Euler and continuity equations of fluids with rotational motion can also be given the form of a generalized Schrödinger equation, in which the vorticity terms appears as an exterior vectorial field. Namely, in this case this equation is similar to the electromagnetic Schrödinger equation.

The nonlinear Schrödinger-type form is also preserved in the case of the Navier–Stokes equations of a viscous fluid, since one may combine the  $\mathcal{D}$  parameter (that generalizes the Compton length of standard quantum mechanics) and the viscosity coefficient in terms of a new complex parameter.<sup>2,17</sup>

We shall in forthcoming works attempt to take into account these effects in more complete numerical simulations with improved integration schemes, to apply the same general concept to other types of systems, then to lead a real hydrodynamic laboratory experiment.

Provided such an actual experiment succeeds, it could lead to many new applications in several domains: didactic ones (teaching of quantum mechanics), laboratory physics (macroscopic models of quantum systems, simulations of atomic and molecular systems, study of the quantum to classical transition, laboratory astrophysics,<sup>17,18</sup> models of biological-like systems,<sup>19,20</sup> applications to atmosphere and ocean problems — climate, freakwaves,<sup>15</sup> etc.), new technology (development of new devices having some macroscopic quantum-like properties and behavior), self-organization (plasma confinement, control of turbulence, etc.).

## Acknowledgments

The authors gratefully acknowledge very fruitful discussions with Dr. L. Di Menza.

## Appendix A. Finite Difference Formulae

Let us give in this Appendix some finite difference formulas for derivatives and apply them to the calculation of the quantum potential

$$Q = -2\mathcal{D}^2 \frac{\Delta\sqrt{P}}{\sqrt{P}}, \tag{A.1}$$

and of the quantum force

$$F_Q = -\nabla Q. \quad (\text{A.2})$$

We set

$$K = \ln P, \quad H = \nabla \ln P. \quad (\text{A.3})$$

The expressions for the quantum potential and the quantum force become:

$$Q = -\mathcal{D}^2 \left\{ \Delta K + \frac{1}{2} (\nabla K)^2 \right\} = -\mathcal{D}^2 \left\{ \nabla \cdot H + \frac{1}{2} H^2 \right\}, \quad (\text{A.4})$$

$$F_Q = \mathcal{D}^2 \{ \Delta H + (H \cdot \nabla) H \}. \quad (\text{A.5})$$

### A.1. One dimension

A.1.1. *Formulas in one dimension valid up to order  $O[\varepsilon^4]$*

$$f'_0 = \frac{f_{-2} - 8f_{-1} + 8f_1 - f_2}{12\varepsilon} = f'[0] - \frac{1}{30} f^{(5)}[0] \varepsilon^4, \quad (\text{A.6})$$

$$f''_0 = \frac{-f_{-2} + 16f_{-1} - 30f_0 + 16f_1 - f_2}{12\varepsilon^2} = f''[0] - \frac{1}{90} f^{(6)}[0] \varepsilon^4, \quad (\text{A.7})$$

$$f^{(3)}_0 = \frac{f_{-3} - 8f_{-2} + 13f_{-1} - 13f_1 + 8f_2 - f_3}{8\varepsilon^3} = f^{(3)}[0] - \frac{7}{120} f^{(7)}[0] \varepsilon^4, \quad (\text{A.8})$$

where we have set  $f_j = f(x + j\delta x)$ .

A.1.2. *Quantum potential in one dimension*

$$Q = -\mathcal{D}^2 \left\{ K'' + \frac{1}{2} K'^2 \right\} = -\mathcal{D}^2 \left\{ H' + \frac{1}{2} H^2 \right\}. \quad (\text{A.9})$$

A.1.3. *Calculation of the quantum potential up to order  $O[\delta x^4]$*

$$Q_0 = -\mathcal{D}^2 \left\{ \frac{-K_{-2} + 16K_{-1} - 30K_0 + 16K_1 - K_2}{12\delta x^2} - \frac{1}{2} \left( \frac{K_{-2} - 8K_{-1} + 8K_1 - K_2}{12\delta x} \right)^2 \right\}, \quad (\text{A.10})$$

in function of  $K = \ln P$  and

$$Q_0 = -\mathcal{D}^2 \left\{ \frac{H_{-2} - 8H_{-1} + 8H_1 - H_2}{12\delta x} + \frac{1}{2} H_0^2 \right\}, \quad (\text{A.11})$$

in function of  $H = \nabla \ln P$ .

A.1.4. *Quantum force in one dimension*

$$F_0 = \mathcal{D}^2(K^{(3)} + K'K'') = \mathcal{D}^2(H'' + HH'). \quad (\text{A.12})$$

A.1.5. *Calculation of the quantum force up to order  $O[\delta x^4]$*

$$\begin{aligned} F_0 = \mathcal{D}^2 & \left\{ \frac{K_{-3} - 8K_{-2} + 13K_{-1} - 13K_1 + 8K_2 - K_3}{8\delta x^3} \right. \\ & + \left( \frac{-K_{-2} + 16K_{-1} - 30K_0 + 16K_1 - K_2}{12\delta x^2} \right) \\ & \left. \times \left( \frac{K_{-2} - 8K_{-1} + 8K_1 - K_2}{12\delta x} \right) \right\}, \end{aligned} \quad (\text{A.13})$$

in function of  $K = \ln P$ , and

$$\begin{aligned} F_0 = \mathcal{D}^2 & \left\{ \frac{-H_{-2} + 16H_{-1} - 30H_0 + 16H_1 - H_2}{12\delta x^2} \right. \\ & \left. + H_0 \frac{H_{-2} - 8H_{-1} + 8H_1 - H_2}{12\delta x} \right\}, \end{aligned} \quad (\text{A.14})$$

in function of  $H = \nabla \ln P$ .

**A.2. Two dimensions**

A.2.1. *Formulas in two dimensions valid up to order  $O[\varepsilon^4]$  (for  $\delta x = \delta y = \varepsilon$ )*

$$\frac{\partial f_{0,0}}{\partial x} = \frac{f_{-2,0} - 8f_{-1,0} + 8f_{1,0} - f_{2,0}}{12\varepsilon} = f^{(1,0)}[0,0] - \frac{1}{30} f^{(5,0)}[0,0]\varepsilon^4, \quad (\text{A.15})$$

$$\frac{\partial f_{0,0}}{\partial y} = \frac{f_{0,-2} - 8f_{0,-1} + 8f_{0,1} - f_{0,2}}{12\varepsilon} = f^{(0,1)}[0,0] - \frac{1}{30} f^{(0,5)}[0,0]\varepsilon^4, \quad (\text{A.16})$$

$$\begin{aligned} \frac{\partial^2 f_{0,0}}{\partial x^2} &= \frac{-f_{-2,0} + 16f_{-1,0} - 30f_{0,0} + 16f_{1,0} - f_{2,0}}{12\varepsilon^2} \\ &= f^{(2,0)}[0,0] - \frac{1}{90} f^{(6,0)}[0,0]\varepsilon^4, \end{aligned} \quad (\text{A.17})$$

$$\begin{aligned} \frac{\partial^2 f_{0,0}}{\partial y^2} &= \frac{-f_{0,-2} + 16f_{0,-1} - 30f_{0,0} + 16f_{0,1} - f_{0,2}}{12\varepsilon^2} \\ &= f^{(0,2)}[0,0] - \frac{1}{90} f^{(0,6)}[0,0]\varepsilon^4, \end{aligned} \quad (\text{A.18})$$

$$\begin{aligned} \frac{\partial^2 f_{0,0}}{\partial x \partial y} &= \frac{10(f_{1,1} - f_{-1,1} - f_{1,-1} + f_{-1,-1})}{24\varepsilon^2} \\ &+ \frac{f_{2,-1} + f_{-2,1} + f_{-1,2} + f_{1,-2} - (f_{2,1} + f_{-2,-1} + f_{1,2} + f_{-1,-2})}{24\varepsilon^2} \\ &= f^{(1,1)}[0,0] - \frac{1}{180} (6f^{(1,5)}[0,0] + 5f^{(3,3)}[0,0] + 6f^{(5,1)}[0,0])\varepsilon^4, \end{aligned} \quad (\text{A.19})$$

$$\begin{aligned}
 \frac{\partial^3 f_{0,0}}{\partial x^3} &= \frac{f_{-3,0} - 8f_{-2,0} + 13f_{-1,0} - 13f_{1,0} + 8f_{2,0} - f_{3,0}}{8\varepsilon^3} \\
 &= f^{(3,0)}[0,0] - \frac{7}{120} f^{(7,0)}[0,0]\varepsilon^4,
 \end{aligned} \tag{A.20}$$

$$\begin{aligned}
 \frac{\partial^3 f_{0,0}}{\partial y^3} &= \frac{f_{0,-3} - 8f_{0,-2} + 13f_{0,-1} - 13f_{0,1} + 8f_{0,2} - f_{0,3}}{8\varepsilon^3} \\
 &= f^{(0,3)}[0,0] - \frac{7}{120} f^{(0,7)}[0,0]\varepsilon^4,
 \end{aligned} \tag{A.21}$$

$$\begin{aligned}
 \frac{\partial^3 f_{0,0}}{\partial x^2 \partial y} &= \frac{(f_{2,-2} - 8f_{2,-1} + 8f_{2,1} - f_{2,2}) + 16(f_{1,-2} - 8f_{1,-1} + 8f_{1,1} - f_{1,2})}{144\varepsilon^3} \\
 &\quad - \frac{30(f_{0,-2} - 8f_{0,-1} + 8f_{0,1} - f_{0,2})}{144\varepsilon^3} \\
 &\quad + \frac{16(f_{-1,-2} - 8f_{-1,-1} + 8f_{-1,1} - f_{-1,2}) - (f_{-2,-2} - 8f_{-2,-1} + 8f_{-2,1} - f_{-2,2})}{144\varepsilon^3} \\
 &= f^{(2,1)}[0,0] - \frac{1}{90} (3f^{(2,5)}[0,0] + f^{(6,1)}[0,0])\varepsilon^4.
 \end{aligned} \tag{A.22}$$

$$\begin{aligned}
 \frac{\partial^3 f_{0,0}}{\partial x \partial y^2} &= \frac{(f_{-2,2} - 8f_{-1,2} + 8f_{1,2} - f_{2,2}) + 16(f_{-2,1} - 8f_{-1,1} + 8f_{1,1} - f_{2,1})}{144\varepsilon^3} \\
 &\quad - \frac{30(f_{-2,0} - 8f_{-1,0} + 8f_{1,0} - f_{2,0})}{144\varepsilon^3} \\
 &\quad + \frac{16(f_{-2,-1} - 8f_{-1,-1} + 8f_{1,-1} - f_{2,-1}) - (f_{-2,-2} - 8f_{-1,-2} + 8f_{1,-2} - f_{2,-2})}{144\varepsilon^3} \\
 &= f^{(1,2)}[0,0] - \frac{1}{90} (3f^{(5,2)}[0,0] + f^{(1,6)}[0,0])\varepsilon^4,
 \end{aligned} \tag{A.23}$$

where  $f_{i,j} = f(x + i\delta x, y + j\delta y)$ .

### A.2.2. Quantum potential in two dimensions

$$Q = -\mathcal{D}^2 \left\{ \frac{\partial^2 K}{\partial x^2} + \frac{\partial^2 K}{\partial y^2} + \frac{1}{2} \left[ \left( \frac{\partial K}{\partial x} \right)^2 + \left( \frac{\partial K}{\partial y} \right)^2 \right] \right\}, \tag{A.24}$$

$$Q = -\mathcal{D}^2 \left\{ \frac{\partial H_x}{\partial x} + \frac{\partial H_y}{\partial y} + \frac{1}{2} (H_x^2 + H_y^2) \right\}, \tag{A.25}$$

**A.2.3. Calculation of the quantum potential up to order  $O[\varepsilon^4]$**

$$\begin{aligned}
 Q_{0,0} = & -\mathcal{D}^2 \left\{ \frac{-K_{-2,0} + 16K_{-1,0} - 30K_{0,0} + 16K_{1,0} - K_{2,0}}{12\delta x^2} \right. \\
 & + \frac{-K_{0,-2} + 16K_{0,-1} - 30K_{0,0} + 16K_{0,1} - K_{0,2}}{12\delta y^2} \\
 & + \frac{1}{2} \left( \frac{K_{-2,0} - 8K_{-1,0} + 8K_{1,0} - K_{2,0}}{12\delta x} \right)^2 \\
 & \left. + \frac{1}{2} \left( \frac{K_{0,-2} - 8K_{0,-1} + 8K_{0,1} - K_{0,2}}{12\delta y} \right)^2 \right\}, \tag{A.26}
 \end{aligned}$$

in function of  $K = \ln P$ , and

$$\begin{aligned}
 Q_{0,0} = & -\mathcal{D}^2 \left\{ \frac{(H_x)_{-2,0} - 8(H_x)_{-1,0} + 8(H_x)_{1,0} - (H_x)_{2,0}}{12\delta x} \right. \\
 & + \frac{(H_y)_{0,-2} - 8(H_y)_{0,-1} + 8(H_y)_{0,1} - (H_y)_{0,2}}{12\delta y} \\
 & \left. + \frac{1}{2} (H_x)_{0,0}^2 + \frac{1}{2} (H_y)_{0,0}^2 \right\}, \tag{A.27}
 \end{aligned}$$

in function of  $H = \nabla \ln P$ .

**A.2.4. Quantum force in two dimensions**

$$F_x = \mathcal{D}^2 \left\{ \frac{\partial^3 K}{\partial x^3} + \frac{\partial^3 K}{\partial x \partial y^2} + \frac{\partial K}{\partial x} \frac{\partial^2 K}{\partial x^2} + \frac{\partial K}{\partial y} \frac{\partial^2 K}{\partial x \partial y} \right\}, \tag{A.28}$$

$$F_y = \mathcal{D}^2 \left\{ \frac{\partial^3 K}{\partial x^2 \partial y} + \frac{\partial^3 K}{\partial y^3} + \frac{\partial K}{\partial x} \frac{\partial^2 K}{\partial x \partial y} + \frac{\partial K}{\partial y} \frac{\partial^2 K}{\partial y^2} \right\}, \tag{A.29}$$

$$F_x = \mathcal{D}^2 \left\{ \frac{\partial^2 H_x}{\partial x^2} + \frac{\partial^2 H_x}{\partial y^2} + H_x \frac{\partial H_x}{\partial x} + H_y \frac{\partial H_x}{\partial y} \right\}, \tag{A.30}$$

$$F_y = \mathcal{D}^2 \left\{ \frac{\partial^2 H_y}{\partial x^2} + \frac{\partial^2 H_y}{\partial y^2} + H_x \frac{\partial H_y}{\partial x} + H_y \frac{\partial H_y}{\partial y} \right\}. \tag{A.31}$$



A.2.5. Calculation of the quantum force up to order  $O[\varepsilon^4]$ 

$$\begin{aligned}
 (F_{0,0})_x = \mathcal{D}^2 & \left\{ \frac{K_{-3,0} - 8K_{-2,0} + 13K_{-1,0} - 13K_{1,0} + 8K_{2,0} - K_{3,0}}{8\delta x^3} \right. \\
 & + \frac{(K_{-2,2} - 8K_{-1,2} + 8K_{1,2} - K_{2,2})}{144\delta x\delta y^2} \\
 & + \frac{16(K_{-2,1} - 8K_{-1,1} + 8K_{1,1} - K_{2,1})}{144\delta x\delta y^2} \\
 & - \frac{30(K_{-2,0} - 8K_{-1,0} + 8K_{1,0} - K_{2,0})}{144\delta x\delta y^2} \\
 & + \frac{16(K_{-2,-1} - 8K_{-1,-1} + 8K_{1,-1} - K_{2,-1})}{144\delta x\delta y^2} \\
 & - \frac{(K_{-2,-2} - 8K_{-1,-2} + 8K_{1,-2} - K_{2,-2})}{144\delta x\delta y^2} \\
 & + \frac{K_{-2,0} - 8K_{-1,0} + 8K_{1,0} - K_{2,0}}{12\delta x} \\
 & \times \frac{-K_{-2,0} + 16K_{-1,0} - 30K_{0,0} + 16K_{1,0} - K_{2,0}}{12\delta x^2} \\
 & + \frac{K_{0,-2} - 8K_{0,-1} + 8K_{0,1} - K_{0,2}}{12\delta y} \\
 & \times \left( \frac{10(K_{1,1} - K_{-1,1} - K_{1,-1} + K_{-1,-1})}{24\delta x\delta y} \right. \\
 & + \frac{(K_{2,-1} + K_{-2,1} + K_{-1,2} + K_{1,-2})}{24\delta x\delta y} \\
 & \left. - \frac{(K_{2,1} + K_{-2,-1} + K_{1,2} + K_{-1,-2})}{24\delta x\delta y} \right) \left. \right\} \tag{A.32} \\
 (F_{0,0})_y = \mathcal{D}^2 & \left\{ \frac{(K_{2,-2} - 8K_{2,-1} + 8K_{2,1} - K_{2,2})}{144\delta x^2\delta y} \right. \\
 & + \frac{16(K_{1,-2} - 8K_{1,-1} + 8K_{1,1} - K_{1,2})}{144\delta x^2\delta y} \\
 & - \frac{30(K_{0,-2} - 8K_{0,-1} + 8K_{0,1} - K_{0,2})}{144\delta x^2\delta y}
 \end{aligned}$$

$$\begin{aligned}
& + \frac{16(K_{-1,-2} - 8K_{-1,-1} + 8K_{-1,1} - K_{-1,2})}{144\delta x^2 \delta y} \\
& - \frac{(K_{-2,-2} - 8K_{-2,-1} + 8K_{-2,1} - K_{-2,2})}{144\delta x^2 \delta y} \\
& + \frac{K_{0,-3} - 8K_{0,-2} + 13K_{0,-1} - 13K_{0,1} + 8K_{0,2} - K_{0,3}}{8\delta y^3} \\
& + \frac{K_{-2,0} - 8K_{-1,0} + 8K_{1,0} - K_{2,0}}{12\delta x} \\
& \times \left( \frac{10(K_{1,1} - K_{-1,1} - K_{1,-1} + K_{-1,-1})}{24\delta x \delta y} \right. \\
& + \frac{K_{2,-1} + K_{-2,1} + K_{-1,2} + K_{1,-2}}{24\delta x \delta y} \\
& \left. + \frac{(K_{2,1} + K_{-2,-1} + K_{1,2} + K_{-1,-2})}{24\delta x \delta y} \right) \\
& + \frac{K_{0,-2} - 8K_{0,-1} + 8K_{0,1} - K_{0,2}}{12\delta y} \\
& \times \left. \frac{-K_{0,-2} + 16K_{0,-1} - 30K_{0,0} + 16K_{0,1} - K_{0,2}}{12\delta y^2} \right\}, \tag{A.33}
\end{aligned}$$

in function of  $K = \ln P$ .

The generalization to three dimensions is straightforward.

## References

1. L. Nottale, Proc. 7th Int. Colloquium on Clifford Algebra, Toulouse, France, May 19–29, 2005, *Advances in Applied Clifford Algebra* **18**, 917 (2008).
2. L. Nottale, *J. Phys. A: Math. Theor.* **42**, 275306 (2009).
3. L. Nottale, *Scale Relativity and Fractal Space-Time: A New Approach to Unifying Relativity and Quantum Mechanics* (Imperial College Press, London, 2011).
4. D. Bohm, *Phys. Rev.* **85**, 166 (1952).
5. L. Nottale, *Fractal Space-Time and Microphysics: Towards a Theory of Scale Relativity* (World Scientific, Singapore, 1993).
6. M. N. Célérier and L. Nottale, *J. Phys. A: Math. Gen.* **37**, 931 (2004).
7. E. Madelung, *Zeit. F. Phys.* **40**, 322 (1927).
8. E. Schrödinger, *Naturwiss.* **14**, 664 (1926).
9. L. I. Schiff, *Quantum Mechanics* (McGraw-Hill, 1968), p. 74.
10. L. Landau and E. Lifchitz, *Quantum Mechanics* (Mir, Moscow, 1967).
11. W. H. Press, B. P. Flannery, S. A. Teukolsky and W. T. Vetterling, *Numerical Recipes* (Cambridge University Press, Cambridge, 1984).
12. L. Landau and E. Lifchitz, *Fluid Mechanics* (Mir, Moscow, 1988).
13. C. Nore, M. E. Brachet, E. Cerda and E. Tirapegui, *Phys. Rev. Lett.* **72**, 2593 (1994).

14. I. H. Hutchinson, *Principles of Plasma Diagnostics* (Cambridge University Press, Cambridge, 2002).
15. L. Nottale, arXiv: 0901.1270.
16. A. L. Fetter, *Phys. Rev. A.* **138**, 429 (1965).
17. L. Nottale, *Astron. Astrophys.* **327**, 867 (1997).
18. L. Nottale, G. Schumacher and E. T. Lefèvre, *Astron. Astrophys.* **361**, 379 (2000).
19. L. Nottale, *Am. Inst. of Phys. Conference Proceedings* **718**, 68 (2004).
20. L. Nottale and C. Auffray, *Prog. Biophys. Mol. Biol.* **97**, 115 (2008).